Chemical Physics Letters 677 (2017) 92–98

Contents lists available at ScienceDirect

Chemical Physics Letters

journal homepage: www.elsevier.com/locate/cplett

Research paper

Configuration interaction study of electronic structures of CdCl including spin-orbit coupling

Shutao Zhao [a,b,*], Jicheng Cui [b], Rui Li [c], Bing Yan [d,*]

[a] School of Physics and Electronic Science, Fuyang Normal College, Fuyang 236037, China
[b] Changchun Institute of Optics, Fine Mechanics and Physics, Chinese Academy of Sciences, Changchun 130033, China
[c] Department of Physics, College of Science, Qiqihar University, Qiqihar 161006, China
[d] Jilin Provincial Key Laboratory of Applied Atomic and Molecular Spectroscopy, Institute of Atomic and Molecular Physics, Jilin University, Changchun 130012, China

ARTICLE INFO

Article history:
Received 16 January 2017
In final form 3 April 2017
Available online 4 April 2017

ABSTRACT

Adiabatic potential energy curves (PECs) and the dipole moments (DMs) for the 14 low-lying Λ-S states of CdCl were computed at configuration interaction method including Davidson correction (+Q). To quantitatively evaluate the spin-orbit coupling (SOC) effect, the SOC integrals involving the $X^2\Sigma^+$ and $2^2\Sigma^+$ were investigated. The spectroscopic constants of 9 bound Λ-S states and 4 lowest bound Ω states were derived. Moreover, the radiative lifetimes of the vibrational levels of bound states were predicted for the first time. Finally, the feasibility and challenges of laser cooling of CdCl were discussed based on a three-laser cooling scheme.

1. Introduction

Due to their import role in environment pollution and chemical reactions, recently the cadmium halides have attracted considerable research interest, which can help us understand how the cadmium-containing species are released into the environment. [1,2] As one of simple cadmium mono-halides, the CdCl molecule can be found in the gas–phase reactions Cd + XCl → CdCl + X (X = H,O,Cl,Br) and Cd_2Cl_2 → 2CdCl, which are involved in the global Cd-recovering [3]. Another motivation is seeking the candidates of molecular laser cooling. The cadmium halides have similar valence electronic structure with SrF molecule [4], which is the first experimentally laser-cooled molecule, if the 3d semi core orbitals are fully occupied. Thus, the detailed information of low-lying electronic states should be examined.

In previous study, some theoretical and experimental efforts on the electronic structure and spectroscopy have been made [5–8]. The spectroscopy of CdCl molecule was first observed by Walter et al. in the 1920s [5]. They made several experimental investigations of the vapours of cadmium and gave three band groups (3018–3074, 3077–3104, 3115–3181 Å) in the absorption spectrum, which were ascribed to the absorption transition $^2\Pi \leftarrow X^2\Sigma^+$ in CdCl. Wieland [6] recorded the emission bands in the infrared and visible spectral range of 3333–8695 Å, corresponding to the spectral band of $B^2\Sigma^+ \rightarrow X^2\Sigma^+$, which was originally, incorrectly ascribed to the spectra of $CdCl_2$. Later, Cornell [7] obtained the spectra in the range of 2185–2240 Å by high frequency discharge, and assigned to an emission transition from the higher excited state $^2\Sigma^+$ to $X^2\Sigma^+$. According to the observed band systems, harmonic vibrational frequency ω_e and anharmonic term $\omega_e x_e$ of the ground state $X^2\Sigma^+$ were determined as 330.5 and 1.2 cm^{-1}, respectively.

Comparing with considerably less experimental studies on CdCl, there have been several theoretical works on the electronic structure using Hartree-Fock (HF), second-order Møller-Plesset perturbation theory (MP2), density functional theory (DFT) and coupled cluster singles and doubles method with a perturbative treatment of triple excitations (CCSD(T)) method. All the theoretical efforts made to date were focused on the ground state $X^2\Sigma^+$ of CdCl. In 1994, Kaupp et al. obtained bond lengths of the $X^2\Sigma^+$ as 2.395 or 2.369 Å with HF and MP2 methods [9]. In their molecular calculations, the 20-valence-electron and 7-valence-electron pseudopotentials were used for the Cd and Cl, respectively. Later, Liao et al. carried out local DFT calculations and predicted the bond length, force constant and vibrational frequency of the ground state $X^2\Sigma^+$ [10]. In their study, only the valence electrons (3 s, 3p of the Cl; 4d, 5 s of the Cd) were allowed to relax. In 2006, Shepler et al. also studied the molecular structures, vibrational frequencies and dissociation energy of the ground state $X^2\Sigma^+$ at CCSD(T) level with the complete basis set (CBS) limit, as well as effects of the

* Corresponding authors at: School of Physics and Electronic Science, Fuyang Normal College, Fuyang 236037, China (S. Zhao), and Jilin Provincial Key Laboratory of Applied Atomic and Molecular Spectroscopy, Institute of Atomic and Molecular Physics, Jilin University, Changchun 130012, China (B. Yan).

E-mail addresses: zhaoshutao2002@163.com (S. Zhao), yanbing@jlu.edu.cn (B. Yan).

http://dx.doi.org/10.1016/j.cplett.2017.04.003
0009-2614/

core-valence (CV) correlation, the spin-orbit coupling (SOC), and the scalar relativity were all taken into account to predict the accurate equilibrium structures and spectroscopic constants [8]. For the ground state $X^2\Sigma^+$, the Shepler's results are the most accurate to date. However, for the excited states of CdCl observed in the previous experiments have not been studied theoretically.

In our present work, theoretical investigations of the electronic structure and transition properties were made on the low-lying electronic states of CdCl, using high level *ab initio* calculations. In the calculations, the CV correlations and SOC effect were taken into accounted, which can play import roles in the spectroscopic characters of the electronic states [11–13]. The PECs of the 14 Λ-S states associated with the two lowest dissociation limits of CdCl, as well as the 30 Ω states correlated with eight lowest dissociation limits were obtained. On the basis of the computed PECs, the spectroscopic parameters of the 9 bound Λ-S and 4 Ω states were determined, most of which were not presented in the previous theoretical reports. The transition properties of the low-lying bound states to the ground state transitions were studied and the radiative lifetimes of the six low-lying vibrational levels of bound states were deduced. Finally, outlining laser cooling scheme for CdCl was presented.

2. Methods

In this study, we performed high-level *ab initio* calculations on the CdCl molecule by using the MOLPRO 2012 software package [14]. In the current electronic structure calculation of the CdCl molecule, the orbital and spin angular momentums are coupled for the Ω state and uncoupled for the Λ-S state. The symmetry group of CdCl is $C_{\infty v}$. Owing to the limit of MOLPRO, the C_{2v} symmetry was used in the electronic structure calculations. The correlations of the irreducible representations between $C_{\infty v}$ and C_{2v} are as follows: $\Sigma^+ = A_1$, $\Pi = B_1 + B_2$, $\Delta = A_1 + A_2$ and $\Sigma^- = A_2$. For the heavy atom Cd, the contracted Gaussian-type basis sets aug-cc-pwCVQZ-PP associated with relativistic effective core potential ECP28MDF [15] were employed, in which the 28 inner electrons are described by a pseudopotential. For the Cl atom, the correlation consistent aug-cc-pVQZ [16] basis sets were chosen. The state-averaged complete active space self-consistent field (CASSCF) [17,18] approach was used to achieve the multi-configuration wavefunctions and subsequently the internally contracted multi-reference configuration interaction including Davidson correction (icMRCI + Q) method [19,20] was used to estimate the dynamical electrons correlations. In CASSCF calculations, the active space consists of seven electrons (Cd $5s^2$ and Cl $3p^5$) in seven molecular orbitals (MOs) which correspond to the 5s5p(Cd) and 3p(Cl) atomic orbitals. The 3 s orbital was kept doubly occupied in CASSCF step, while in the following icMRCI + Q calculations, the twelve electrons (Cd $4d^{10}$ and Cl $3s^2$) were included to account for the CV correlations. That's all the nineteen electrons were correlated in the icMRCI + Q calculations. Finally, the SOC effect was taken into consideration with state-interacting approach using ECP spin-orbit operator for Cd and the Breit-Pauli operator for Cl [21–23]. A similar two-step procedure employed in previous theoretical studies [24–26] was used in our present work, where the SOC effect was treated as a perturbation. The diagonal matrix elements in spin-orbit Hamiltonian were replaced by the icMRCI + Q energy of Λ-S state, and the off-diagonal matrix elements were generated from icMRCI wavefunctions. At the same time, we also focus the perturbation of the electronic states arising from the SOC effect. And the spin-orbit matrix element is required for the quantificational description of the interaction.

On the basis of the calculated PECs of the Λ-S and Ω states, Einstein coefficients and Franck-Condon factors (FCFs) for the $2^2\Pi$-$X^2\Sigma^+$, $2^2\Sigma^+$-$X^2\Sigma^+$, (2)3/2-(1)1/2 and (3)1/2-(1)1/2 bands were obtained with the help of the LEVEL program [27]. Finally, the radiative lifetimes of the six lowest vibrational levels of bound states were computed from these data.

3. Results and discussion

3.1. PECs of Λ-S states

The spin-free PECs of 14 Λ-S states were computed at MRCI + Q level with the step size set at 0.05 Å for R = 1.8–3.8, 0.1 Å for R = 3.8–4.5, 0.5 Å for R = 4.5–5.0, and 1.0 Å for R = 5.0–7.0, which were illustrated in Fig. 1. The first dissociation asymptote Cd(^{1}S) + Cl(^{2}P) correlated with the ground state $X^2\Sigma^+$ and the $1^2\Pi$ state. The second dissociation asymptote Cd(^{3}P) + Cl(^{2}P) correlates with two $^{2,4}\Sigma^+$, one $^{2,4}\Sigma^-$, two $^{2,4}\Pi$, and one $^{2,4}\Delta$ lying at 30147 cm^{-1} above the first asymptote, which agrees well with the experimental value [28] of 31246 cm^{-1}. The $X^2\Sigma^+$, $2^2\Sigma^+$, $3^2\Sigma^+$, $2^2\Pi$, $1^2\Delta$, $1^2\Sigma^-$, $1^4\Sigma^+$, $1^4\Delta$ and $1^4\Sigma^-$ states are typical bound and quasibound states, of which the corresponding spectroscopic constants were given in Table 1.

Because of the ECP28MDF effective core potentials employed in this work, the 28 inner electrons of Cd atom were treated by pseudopotential, hence, the n = 1–3 shells were not included in the MOs. The 1–7σ, 1δ, and 1–3π MOs are constructed from the Cd 4s4p4d and Cl 1s2s2p3s orbitals, which are doubly occupied. The 8σ and 9σ are bonding and anti-bonding, respectively, constructed mainly from the $3p_z$ of Cl and 5 s of Cd. The $5p_z$ of Cd makes a main contribution to the 10σ orbital, which is more diffuse than 8–9σ orbitals. The 4π and 5π MOs are almost completely from Cl $3p_x3p_y$ and Cd $5p_x5p_y$ atomic orbitals, respectively.

As listed in Table 1, the ground state $X^2\Sigma^+$ originating the electronic configuration $8\sigma^2 9\sigma^1 4\pi^4$ (85%) has the values of 328.6 cm^{-1} for ω_e with the error of 2.4 cm^{-1} (0.7%) differing from the experimental results [29], which is also qualitative agreement with the latest theoretical predictions [8] 334.7 cm^{-1} with the error of 1.8%. The value of $\omega_e x_e$ and D_e are computed to be 1.24 cm^{-1} and 1.8 eV, which differ from the experimental value [29] by 0.24 cm^{-1} and ~0.3 eV, respectively. The experimental values D_e were obtained from absorption spectrum with temperature dependence, which are in the range of 1.3–2.1 eV with a large uncertainty. Our computational result D_e falls in the error bar of experimental value, and is in good agreement with the latest theoretical result 1.89 eV [8]. For R_e, several theoretical values were reported, which are 2.3329 (CCSD(T)) [8], 2.38 (DFT) [10] and

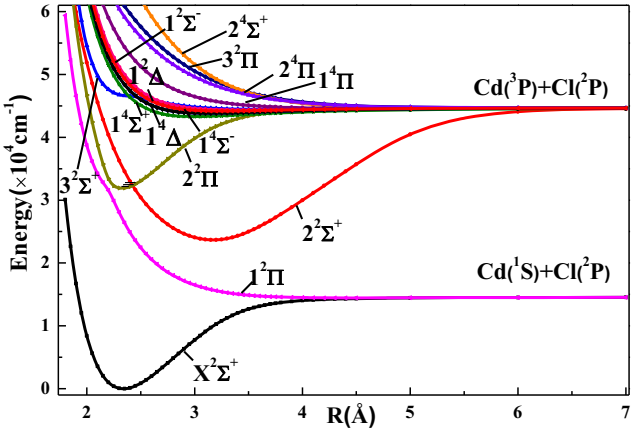

Fig. 1. MRCI + Q potential energy curves of 14 Λ-S states related to the first and second dissociation asymptotes of CdCl molecule. The v = 0–2 vibrational levels of $2^2\Pi$ state are indicated.

Table 1
Spectroscopic constants of the Λ-S states of CdCl.

State		T_e (cm^{-1})	ω_e (cm^{-1})	$\omega_e x_e$ (cm^{-1})	B_e (cm^{-1})	R_e (Å)	D_e (eV)	Configuration at R_e (%)
$X^2\Sigma^+$	This work	0	328.58	1.2447	0.1156	2.3397	1.8018	$8\sigma^2 9\sigma^1 4\pi^4$ (85)
	Expt.[a]		331.0	1.0			1.3–2.1	
	Calc.[b]		334.7			2.3329	1.8907	
	Calc.[c]		305			2.38		
	Calc.[d]					2.369		
$2^2\Sigma^+$		23669	182.32	0.2349	0.0629	3.1706	2.5879	$8\sigma^1 9\sigma^2 4\pi^4$ (76)
$2^2\Pi$		31905	384.44	1.5801	0.1171	2.3251	1.5751	$8\sigma^2 4\pi^4 5\pi^1$ (75)
	Expt.[a]	32163[e]	399.0	1.5				
$3^2\Sigma^+$		44419	25.46	0.8036		3.7829	0.0253	$8\sigma^2 9\sigma^1 4\pi^3 5\pi^1$ (65)
$1^4\Sigma^+$		43297	85.403	1.6015	0.0703	2.9994	0.1621	$8\sigma^2 9\sigma^1 4\pi^3 5\pi^1$ (99)
$1^4\Delta$		43833	67.99	1.5103	0.0652	3.1155	0.0996	$8\sigma^2 9\sigma^1 4\pi^3 5\pi^1$ (99)
$1^4\Sigma^-$		44190	51.43	1.4571	0.0595	3.2624	0.0564	$8\sigma^2 9\sigma^1 4\pi^3 5\pi^1$ (98)
$1^2\Delta$		44090	49.33	1.1779	0.0572	3.3254	0.0652	$8\sigma^2 9\sigma^1 4\pi^3 5\pi^1$ (99)
$1^2\Sigma^-$		44325	38.79	1.1919	0.0529	3.4578	0.0386	$8\sigma^2 9\sigma^1 4\pi^3 5\pi^1$ (99)

[a] Ref. [29].
[b] Ref. [8].
[c] Ref. [10].
[d] Ref. [9].
[e] Ω-averaged experimental value.

2.369 Å (MP2) [9]. The CCST(T) result is excellent agreement with our present value 2.3397 Å, and the others are in similar quality.

The $2^2\Sigma^+$ state originates from the electronic configuration $8\sigma^1 9\sigma^2 4\pi^4$ (76%), corresponding the one-electron transition from 8σ to 9σ orbital. In previous experiments, Wieland assigned the observed unclassified and complicated emission bands in the range of 11500–30000 cm^{-1} to the $^2\Sigma^+ \rightarrow X^2\Sigma^+$ transition in CdCl [6]. As shown in Fig. 1, electronic transitions $2^2\Sigma^+ \rightarrow X^2\Sigma^+$ and $2^2\Pi \rightarrow X^2\Sigma^+$ can be allowed satisfying the conditions $\Delta\Lambda = 0$ and +1, which led to the continuous and discrete emission spectrum. Because of the large difference in the equilibrium bond distance R_e between $2^2\Sigma^+$ and $X^2\Sigma^+$, the hot bands arising from $2^2\Sigma^+ \rightarrow X^2\Sigma^+$ transition are distributed in a large range. Our calculated T_e of $2^2\Sigma^+$ is 23669 cm^{-1}, which is exactly in the experimentally observed spectral range, therefore, the $^2\Sigma^+ \rightarrow X^2\Sigma^+$ transition in previous experiment should be the $2^2\Sigma^+ \rightarrow X^2\Sigma^+$ transition in our work. Our theoretically computed spectroscopic constants T_e, ω_e and $\omega_e x_e$ for the $2^2\Sigma^+$ values were 23669, 182.3 and 0.23 cm^{-1}, respectively, which are reasonably agree with those obtained by Patel et al. [30] in early experiment, 26010, 153.5 and 3.75 cm^{-1}, respectively. The D_e of $2^2\Sigma^+$ is predicted to be 2.59 eV, indicating strong bonding character for this state.

The $2^2\Pi$ state arises from the electronic configuration $8\sigma^2 4\pi^4 5\pi^1$ (75%) corresponding the one-electron transition from $9\sigma \rightarrow 5\pi$. The values of T_e, ω_e and $\omega_e x_e$ are calculated to be 31905, 384 and 1.58 cm^{-1}, respectively, in good agreement with the experimental values [29] 32163, 399 and 1.5 cm^{-1}. The predicted well depth of $2^2\Pi$ state is 1.58 eV, which is shallow than those of the two lower states $2^2\Sigma^+$ and ground state. The repulsive $1^2\Pi$ state originates from the electronic configuration $8\sigma^2 9\sigma^2 4\pi^3$ (90%), corresponding the one-electron transition from 4π to 9σ orbital. An avoided-crossing point between repulsive $1^2\Pi$ and bound $2^2\Pi$ states is located at the region R = 2.2 Å, where the main configurations for these two $^2\Pi$ states present abrupt changes, leading to the exchange of their dominant configurations. The main configuration of $3^2\Sigma^+$ is $8\sigma^2 9\sigma^1 4\pi^3 5\pi^1$ (65%) arising from the one-electron transition from 4π to 5π. The spectroscopic values are calculated to be 44419, 25.5 and 0.8 cm^{-1} for T_e, ω_e and $\omega_e x_e$, respectively. And the computed R_e of this state is 3.78 Å, which differs from that of ground state by ~2 Å, indicating that only vertical emission from $3^2\Sigma^+$ to high vibrational levels of $X^2\Sigma^+$ could be observed. The spectra range of this emission is around ~40000 cm^{-1}. In previous experiment [29], a bound $^2\Sigma^+$ state lying 45398 cm^{-1} above ground state was observed, while the spectroscopic constant differs greatly from those of presently computed $3^2\Sigma^+$ state. Therefore, the experimentally observed $^2\Sigma^+$ state should not be assigned as the $3^2\Sigma^+$ state. It is should be noted that a shoulder located at R = 2.45 Å is found on the PEC of $3^2\Sigma^+$ state. The potential shoulder should be formed by avoided crossing with an upper $3^2\Sigma^+$ state, which was not included in this work. The experimentally observed $^2\Sigma^+$ state with T_e = 45398 cm^{-1} should be a higher bound state rather than $3^2\Sigma^+$ state. Three bound quartet states $1^4\Sigma^+$, $1^4\Delta$ and $1^4\Sigma^-$ are found in our calculations. The $1^4\Sigma^+$ state is the lowest one, lying 43297 cm^{-1} above the ground state $X^2\Sigma^+$ with R_e = 2.9994 Å. Compared with the values of the $1^4\Sigma^+$ state, the transition energies (T_e) of the $1^4\Delta$ and $1^4\Sigma^-$ states are 536 and 893 cm^{-1} higher, and the values of R_e for these two states are 0.1161 and 0.263 Å larger, respectively. All three quartet states mentioned above have the common configuration $8\sigma^2 9\sigma^1 4\pi^3 5\pi^1$, which corresponds to single-electron excitation from the 4π to the 5π molecular orbital. As such these quartet states could be metastable because of the forbidden transitions of these states to the ground state. Since no previous spectroscopic constants have been reported for the $1^2\Delta$, $1^2\Sigma^-$ and these bound quartet states, our computed spectroscopic constants of these states could provide more useful information for the further experimental investigations.

As shown in Fig. 1, the $2^2\Sigma^+$ state has a deep minimum at R = 3.1706 Å, owing to strong interaction between $2^2\Sigma^+$ and the $X^2\Sigma^+$. Similarly, an avoided crossing point can be found near R = 2.2 Å between $1^2\Pi$ and $2^2\Pi$ state with the same symmetry. The $1^2\Pi$ state is unbound but has a shoulder near the avoided crossing region, and the $2^2\Pi$ state also has a deep minimum at R = 2.3251 Å caused by the avoided crossing.

For these spin-free Λ-S states, the DMs at MRCI + Q level were also computed and given in Fig. 2. The configurations and polarity of these states were discussed with the aid of the DMs. In the equilibrium bond length R = 2.35 Å, our predicted absolute DM of the $X^2\Sigma^+$ state is 1.06 a.u. which is slightly smaller but quantitatively consistent with that of isovalent molecule ZnCl (1.29 a.u.) [31], and the leading configuration of this state is $8\sigma^2 9\sigma^1 4\pi^4$, correlating to a single electron transfer from Cd 5s to Cl 3p, revealing that ground state CdCl has ionic character. The absolute DM reaches the largest value around R = 2.85 Å and then decreases to zero at longer distance R > 4.5 Å, correlating with the covalent dissociation limit. For distance R > 7 Å, the DM of $2^2\Sigma^+$ tends to be zero, indicating a covalent structure. In the range of R = 2.85–7 Å, the DM of $2^2\Sigma^+$ is negative and its absolute value reach a maximum near R = 4 Å,

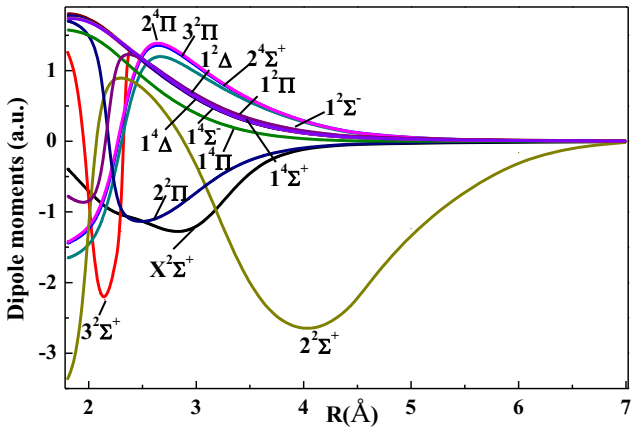

Fig. 2. Evolution of dipole moments of the Λ-S states as a function of internuclear distance of CdCl molecule.

which means that this state has an ionic $Cd^{\delta+}Cl^{\delta-}$ characteristic. In the region near R = 1.95 Å, there a drastic change of DM of the $2^2\Sigma^+$ and $3^2\Sigma^+$ due to the avoided crossing, which means that their ionic characters are exchanged. Such a phenomenon can be found between $1^2\Pi$ and $2^2\Pi$ around R = 2.2 Å, which also indicates an exchange of their polarity.

3.2. PECs of the Ω states

As stated above, the PECs of 14 spin-free Λ-S states were determined by solving the Hamiltonian with the Born-Oppenheimer approximation, while the spin-orbit part was not considered. In this work, the spin-orbit effects were introduced with a two-step perturbation procedure as used in previous theoretical works [24–26]. For the molecule containing high-Z elements, the SOC is of great importance to the spectroscopy and dynamics in laser field as investigated in previous computations [32–41]. As the heavy metal chloride CdCl, the SOC effect can make a strong effect on multiplet state as expected. When the SOC effect is considered, several Ω states can be generated from a given multiplet Λ-S state, therefore, there will be 30 Ω states generated from the 14 spin-free Λ-S states of CdCl, including 15 states of Ω = 1/2, 10 states Ω = 3/2, 4 states of Ω = 5/2, 1 state of Ω = 7/2. The spin-orbit energy separations of $^3P_1$-$^3P_0$ and $^3P_2$-$^3P_0$ of Cd as well as $^2P_{1/2}$-$^2P_{3/2}$ of Cl are calculated to be 525, 1576, and 906 cm^{-1}, respectively, which are in fairly good agreement with the previous experimental values 542, 1713 and 882 cm^{-1} [28].

When the SOC effects are taken into consideration, there will be eight dissociation limits $Cd(^1S_0) + Cl(^2P_{3/2})$, $Cd(^1S_0) + Cl(^2P_{1/2})$, $Cd(^3P_0) + Cl(^2P_{3/2})$, $Cd(^3P_0) + Cl(^2P_{1/2})$, $Cd(^3P_1) + Cl(^2P_{3/2})$, $Cd(^3P_1) + Cl(^2P_{1/2})$, $Cd(^3P_2) + Cl(^2P_{3/2})$, and $Cd(^3P_2) + Cl(^2P_{1/2})$ generated from the previous dissociation asymptotes $Cd(^1S) + Cl(^2P)$ and $Cd(^3P) + Cl(^2P)$. The PECs of the 30 Ω states correlated with eight lowest dissociation limits were plotted in Fig. 3. For clarity, the calculated PECs of the Ω = 1/2, 3/2, 5/2, and 7/2 were presented in the panels (a–d). The spectroscopic parameters of the four low-lying bound Ω states as well as the dominant Λ-S compositions at R_e were determined and given in Table 2. The dominate Λ-S compositions of the $X^2\Sigma^+_{1/2}((1)1/2)$ is the $X^2\Sigma^+$ (99.7%), hence their spectroscopic constants are nearly the same. The computed D_e of $X^2\Sigma^+_{1/2}$ (1.7694 eV) is located in the experimental range of 1.3–2.1 eV, which is 0.03 eV lower than that of the spin-free state $X^2\Sigma^+$ (1.8018 eV).

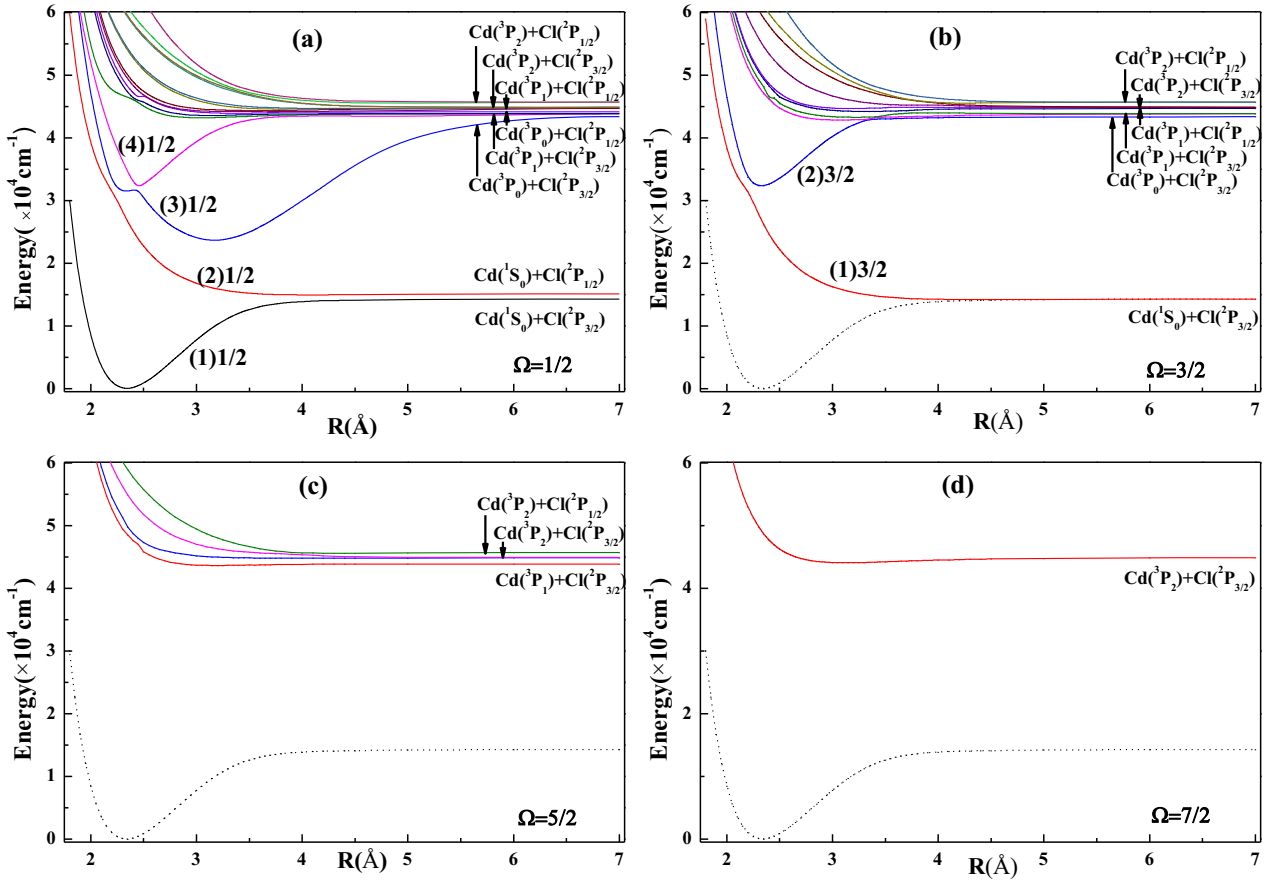

Fig. 3. The potential energy curves of the Ω states of CdCl. (a) Ω = 1/2; (b) Ω = 3/2; (c) Ω = 5/2; (d) Ω = 7/2.

Table 2
Spectroscopic constants of the bound Ω states of the CdCl.

state		T_e (cm^{-1})	ω_e (cm^{-1})	$\omega_e x_e$ (cm^{-1})	B_e (cm^{-1})	R_e (Å)	D_e (eV)	Dominant Λ-S composition at respective R_e (%)
$X^2\Sigma^+_{1/2}$		0	328.54	1.2448	0.1156	2.3397	1.7694	$X^2\Sigma^+$ (99.7)
	Expt.[a]		331.0	1.0			1.3–2.1	
	Calc.[b]		334.7			2.3329	1.8907	
	Calc.[c]		305			2.38		
	Calc.[d]					2.369		
(3) 1/2	Inner well	31480				2.3308		$2^2\Pi_{1/2}$ (99.7)
	Expt.[a]	31485						
	Outer well	23670	182.29	0.2383	0.0629	3.1716	2.4400	$2^2\Sigma^+_{1/2}$ (99.86)
$2^2\Pi_{3/2}$		32351	379.34	1.5046	0.1174	2.3215	1.3651	$2^2\Pi_{3/2}$ (99.78)
	Expt.[a]	32502	399.0	1.5				
(4) 1/2		32135	655.91	18.8384	0.1055	2.4536	1.4526	$2^2\Pi_{1/2}$ (92.7)

[a] Ref. [29].
[b] Ref. [8].
[c] Ref. [10].
[d] Ref. [9].

When the SOC effect is considered, the double multiplet state $2^2\Pi$ splits into two Ω states $2^2\Pi_{1/2}$ and $2^2\Pi_{3/2}$. Because of the common Ω = 1/2 between the $2^2\Pi_{1/2}$ and $2^2\Sigma^+_{1/2}$, the (3)1/2 and (4)1/2 form an avoided crossing at R = 2.45 Å, which results in the (4)1/2 potential well shifting higher by 655 cm^{-1} and the bond-length increasing by 0.1228 Å compared with the inner well of (3)1/2. To further investigate the influence of SOC effect on the PECs, the variations of Λ-S compositions for the Ω = (3)1/2 and (4)1/2 are listed in Table S1 (Supplementary Materials) around the avoided crossing region R = 2.45 Å, where their dominant Λ-S compositions are exchanged for each other. The experimental SOC splitting is 1017 cm^{-1}, our computed value is underestimated by ~150 cm^{-1}. Two local minima on the PEC of (3)1/2 can be found, while the inner well located at 2.3308 Å can support only one vibrational level in our computations, this is maybe the reason that no vibrational spectroscopic constants are available in experiment. In contrast, the vibrational spectroscopic constants of $2^2\Pi_{3/2}$ ((2)3/2) were experimentally determined [29], our computed values are in good agreement with available ones.

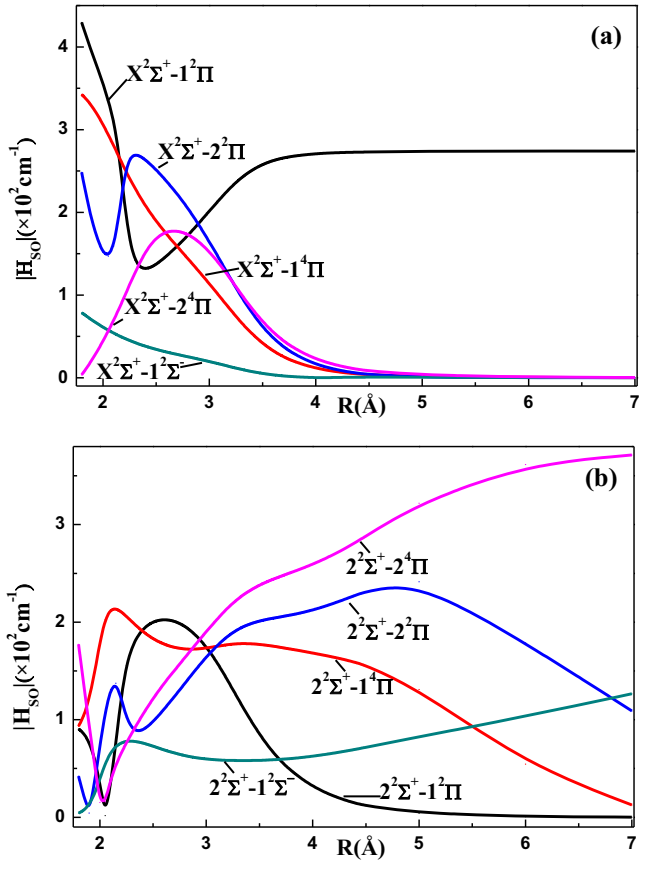

Fig. 4. The absolute R-dependent spin-orbit integrals involving $X^2\Sigma^+$ and $2^2\Sigma^+$ states.

To quantitatively estimate the SO interactions, the SOC integrals involving the $X^2\Sigma^+$ and $2^2\Sigma^+$ states are investigated and displayed in Fig. 4. The SOC integrals including the $1^2\Pi$ and $2^2\Pi$ present irregular behavior, which results from the drastic changes of their electronic configurations around the avoided crossing region R = 2.45 Å mentioned above. The $X^2\Sigma^+$-$1^2\Sigma^-$ and $X^2\Sigma^+$-$1^4\Pi$ coupling monotonically decrease with the increase of the internuclear distance, while the $2^2\Sigma^+$-$2^4\Pi$ monotonically increase for R > 2 Å. In the Franck-Condon region, the $2^2\Sigma^+$-$1^4\Pi$ and $2^2\Sigma^+$-$1^2\Sigma^-$ coupling integrals are near constant, which are about 180 and 75 cm^{-1}, respectively, indicating considerable large SO interactions. At R = 2.4 Å, $2^2\Pi$ crosses with $2^2\Sigma^+$, and the SO-matrix at this point is 90 cm^{-1}, which would lead strong perturbation on the low-lying vibrational level of $2^2\Pi_{1/2}$. Hence, the upper vibrational levels transition from $2^2\Pi_{1/2}$ to $X^2\Sigma^+_{1/2}$ would be perturbed.

3.3. Transition properties and feasibility for laser cooling of CdCl

The TDM functions of $1^2\Pi$-$X^2\Sigma^+$, $2^2\Pi$-$X^2\Sigma^+$ and $2^2\Sigma^+$-$X^2\Sigma^+$ excluding and including the SOC effect were calculated at the internuclear distance R = 1.8–7.0 Å and are shown in Fig. 5(a) and Fig. 5(b), respectively. The TDM of the $2^2\Sigma^+$-$X^2\Sigma^+$ increases with the distance and reach its maximum value at R = 3.25 Å. At short distance R < 2.3 Å, the TDMs of $1^2\Pi$-$X^2\Sigma^+$ have large values, which means that the absorption to repulsive $1^2\Pi$ state may occur with sufficient intensity to produce a continuum background in the absorption spectra. In previous experiment, three groups of spectra bands in the visible region were observed [5], by comparing with present computational results, the electron transition from the $1^2\Pi$ to the ground state are found in this spectral region. In the molecular bonding region, the TDM of the $2^2\Pi$-$X^2\Sigma^+$ has a maximum at R = 2.25 Å and then gradually decreases to zero at larger distance R > 4.5 Å. In generally, the calculated TDMs of $2^2\Pi$-$X^2\Sigma^+$ are predicted to be larger than those of two other transitions in the Franck-Condon region. Moreover, due to the similar equilibrium internuclear distances of the $2^2\Pi$ and $X^2\Sigma^+$ states, the $2^2\Pi$-$X^2\Sigma^+$ transition is the most probable among these transitions. Because of the spin-forbidden transitions ^3P_u-^1S_g for Cd atom, both $2^2\Pi$-$X^2\Sigma^+$ and $2^2\Sigma^+$-$X^2\Sigma^+$ transitions tend to be zero at large internuclear distance. When the SOC effect is considered, there are significant changes on the TDM functions of (3)1/2-(1)1/2 and (4)1/2-(1)1/2 as compared to the $2^2\Pi$-$X^2\Sigma^+$ and $2^2\Sigma^+$-$X^2\Sigma^+$, due to the

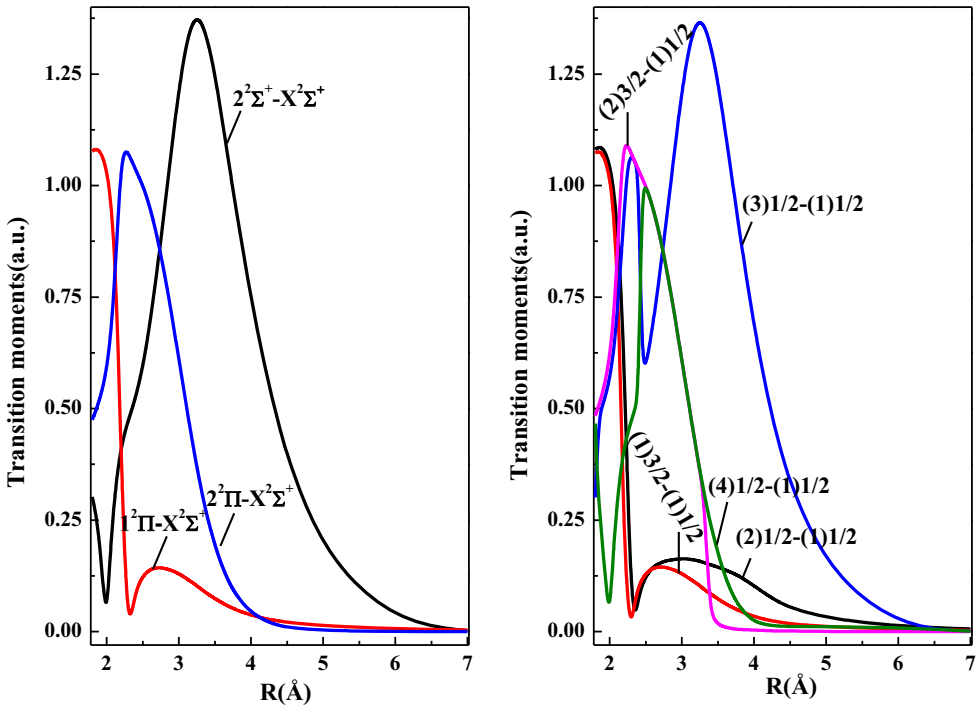

Fig. 5. The absolute transition dipole moments of $1^2\Pi$-$X^2\Sigma^+$, $2^2\Pi$-$X^2\Sigma^+$and $2^2\Sigma^+$-$X^2\Sigma^+$ excluding and including SOC effect as a function of internuclear distance of CdCl molecule.

exchange of wavefunctions between $2^2\Pi$ and $2^2\Sigma^+$ states at the crossing point $R = 2.45$ Å. For the other TDM functions, no significant changes are found in the Franck-Condon region.

The Einstein coefficients $A_{v'v''}$, Franck-Condon factors (*FCFs*) and transition energies $T_{v'v''}$ for the transitions of $2^2\Pi$-$X^2\Sigma^+$, $2^2\Sigma^+$-$X^2\Sigma^+$, (2)3/2-(1)1/2 and (3)1/2-(1)1/2 were estimated and given in Tables S2–S5 (Supplementary Materials), respectively. For the $2^2\Pi$-$X^2\Sigma^+$ and (2)3/2-(1)1/2 transitions, the diagonal Δv $(v'-v'') = 0$ bands tend to be more intense than the other bands. The largest Einstein coefficients occur at the (0,35) and (0,20) bands for the $2^2\Sigma^+$-$X^2\Sigma^+$ and (3)1/2-(1)1/2 transitions, respectively, indicating that these bands are the most intense among all the transition bands studied in this work as a result of the larger differences of equilibrium bond length for $2^2\Sigma^+$ and (3)1/2 states. e for a given vibrational level v' was derived by the inverse of the total Einstein coefficient $A_{v'} = \left(\sum_{v''} A_{v'v''}\right)$. On the basis of the computed Einstein coefficients $A_{v'v''}$, the radiative lifetimes of the low vibrational levels $v' = 0$–5 of bound states were acquired and listed in Table S6 (Supplementary Materials). There are two wells on the PEC of (3)1/2, the inner and outer wells correlate the $2^2\Pi_{1/2}$ and $2^2\Sigma^+_{1/2}$, respectively. As mentioned above, the inner well $2^2\Pi_{1/2}$ can support only one vibrational level, so, the radiative lifetime of the only vibrational level $v' = 0$ is found. The radiative lifetimes of low-lying vibrational levels of $2^2\Sigma^+$ and $2^2\Sigma^+_{1/2}$ are almost the same, which are on the order of hundred nanoseconds. However, the corresponding radiative lifetimes of $2^2\Pi_{3/2}$ increase with respect to that of $2^2\Pi$, which are on the order of ten nanoseconds.

As listed in Table S2 (Supplementary Materials), the Franck-Condon factors (FCFs) for vibrational transitions of $2^2\Pi$-$X^2\Sigma^+$ are highly diagonal, the FCFs of 0–0, 1–1, and 2–2 transitions are $f_{00} = 0.9795$, $f_{11} = 0.9535$, and $f_{22} = 0.9482$, respectively. This is an important criterion to select the laser cooling candidates of diatomic molecules, which ensures limited numbers of laser required in a close-loop cooling cycle. In present laser cooling scheme for CdCl molecule, only three cooling lasers in ultraviolet region, including one main pump laser with $\lambda_{00} = 313.2$ nm and two repump lasers with $\lambda_{10} = 316.4$ nm and $\lambda_{21} = 315.9$ nm, are required, as shown in Fig. 6. The main cooling transition would be $X^2\Sigma^+$ $(v'' = 0) \rightarrow 2^2\Pi(v' = 0)$, the molecules populating in the $2^2\Pi(v' = 0)$ spontaneously decay to the $X^2\Sigma^+(v'' = 0)$ with large probability (0.9795), and to the $X^2\Sigma^+(v'' = 1)$ with small probability (0.0193). And the total probability of the decays to $v'' = 2$ and 3^+ from $2^2\Pi$ $(v' = 0)$ is less than 10^{-3}. Two repump lasers are required to excite the molecules populating on the $v'' = 1$ and $v'' = 2$ of ground state into the $v' = 0$ and $v' = 1$ of $2^2\Pi$ state, respectively. The values of f_{03} and f_{13} are in 10^{-4} and 10^{-3} order of magnitude, respectively, indicating another repump laser is not required. The lifetime of $2^2\Pi$ state is ~13 ns, which is almost the same with that of SrF, ensuring the significant rate of optical cycling in present laser cooling scheme.

While some challenges for laser cooling of CdCl molecule still exist. As shown in Fig. 1, the repulsive state $1^2\Pi$ just lies below the $2^2\Pi$ state, and nonadiabatic coupling among 1–$2^2\Pi$ states may exist around the avoided crossing point. Transitions from $2^2\Pi$ state to the $1^2\Pi$ state, adiabatically or nonadiabatically, would lead dissociation of CdCl along repulsive PEC of $1^2\Pi$ state, and ground-state Cd and Cl atoms would be produced. The released kinetic energy may be transferred and reproduce hot CdCl molecule via collision process. Another difficulty is that the possible perturbation to the $2^2\Pi$ state coming from the interaction with the $2^2\Sigma^+$ state. The $2^2\Sigma^+$ state is a bound one, and the crossing point with $2^2\Pi$ state is located at the classical turning point of $v = 1$ of $2^2\Pi$ state. The spin-orbit matrix between $2^2\Pi$ state and $2^2\Sigma^+$ state is about 100 cm^{-1}, indicating possible predissociation pathway induced by spin-orbit interaction may be opened, and there is a small probability that the molecule is trapped in the potential well of $2^2\Sigma^+$ state. And since strong transition between $2^2\Sigma^+$ state and ground state exists, fast decays to ground state will occur. This is another channel that produce hot CdCl molecule.

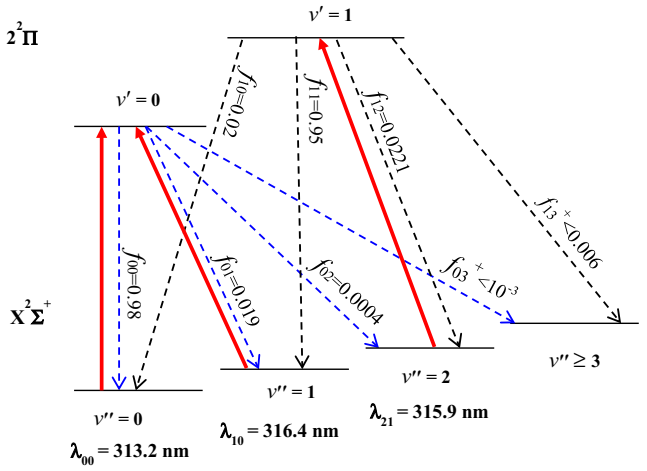

Fig. 6. Proposed laser cooling scheme for CdCl employing the $X^2\Sigma^+ \rightarrow 2^2\Pi$ transition (solid line) and decay pathways (dotted line) with calculated $f_{v'v''}$. Here $\lambda_{v'v''}$ is the wavelength of the $X^2\Sigma^+(v'') \rightarrow 2^2\Pi(v')$ transition.

Both of the above two channel will generate more hot molecules, and thus the efficiency of the laser-cooling scheme would be lowered.

4. Conclusions

The PECs of 14 Λ-S states of CdCl correlated with the two lowest dissociation limits and the DMs of these states were calculated at MRCI level. From the computed PECs, we found that there are nine bound and quasibound states $X^2\Sigma^+$, $2^2\Sigma^+$, $3^2\Sigma^+$, $2^2\Pi$, $1^2\Delta$, $1^2\Sigma^-$, $1^4\Sigma^+$, $1^4\Delta$ and $1^4\Sigma^-$ states as well as five repulsive states $1^2\Pi$, $3^2\Pi$, $2^4\Sigma^+$, $1^4\Pi$ and $2^4\Pi$, of which 8 excited bound states have not been characterized so far. The spectroscopic constants of these bound Λ-S states and 4 lowest bound Ω states were determined, which show, in general, good agreement with the experimental results. The (3)1/2 and 4(1/2) form an avoided crossing at R = 2.45 Å, where the dominant Λ-S compositions of Ω = (3)1/2 and (4)1/2 are exchanged for each other. To quantitatively evaluate the SO interactions, the SOC integrals involving the $X^2\Sigma^+$ and $2^2\Sigma^+$ were obtained. The TDMs, Einstein coefficients and Franck-Condon factors of the transitions $2^2\Pi$-$X^2\Sigma^+$, $2^2\Sigma^+$-$X^2\Sigma^+$, (2)3/2-(1)1/2 and (3)1/2-(1)1/2 were derived, from which the radiative lifetimes of these transitions (v' = 0–5) were predicted to be on the order of ten or hundred nanoseconds. Finally, the feasibility for laser cooling of CdCl was discussed based on a three-laser cooling scheme, and simultaneously, the challenges in laser cooling of CdCl molecule was also presented. Our present theoretical studies reveal more information on the spectroscopic properties of the excited states for CdCl molecule. And the Group IIB halides may become new molecular candidates for laser cooling.

Acknowledgments

This work was supported by National Natural Science Foundation of China (Grant Nos. 11604052, 11404180 and 11574114); the Natural Science Foundation of Heilongjiang Province, China (Grant No. A2015010); Natural Science Foundation of Jilin Province, China (Grant No. 20150101003JC); University Nursing Program for Young Scholars with Creative Talents in Heilongjiang Province, China (Grant No. UNPYSCT-2015095) and the fund of the National Engineering Research Center for Diffraction Gratings Manufacturing and Application, Changchun Institute of Optics, Fine Mechanics and Physics, China (Grant Nos. K201601 and K201701).

Appendix A. Supplementary material

Supplementarydata associated with this article can be found, in the online version, at http://dx.doi.org/10.1016/j.cplett.2017.04.003.

References

[1] L.Q. Ma, G.N. Rao, J. Environ. Qual. 26 (1997) 259.
[2] A.A. Olajire, E.T. Ayodele, G.O. Oyedirdan, E.A. Oluyemi, Environ. Monit. Assess. 85 (2003) 135.
[3] C.R. Williams, R.M. Harrison, Experientia 40 (1984) 29.
[4] E.S. Shuman, J.F. Barry, D. DeMille, Nature 467 (2010) 820.
[5] J.M. Walter, S. Barratt, Proc. R. Soc. Lon. A 122 (1929) 201.
[6] K. Wieland, Helv. Phys. Acta 2 (1929) 46.
[7] S.D. Cornell, Phys. Rev. 54 (1938) 341.
[8] B.C. Shepler, K.A. Peterson, J. Phys. Chem. A 110 (2006) 12321.
[9] M. Kaupp, H.G. von Schnering, Inorg. Chem. 33 (1994) 4179.
[10] M. Liao, Q. Zhang, W.H.E. Schwarz, Inorg. Chem. 34 (1995) 5597.
[11] S. Li, R. Zheng, S.J. Chen, Q.C. Fan, Mol. Phys. 113 (2015) 1433.
[12] L.L. Zhang, S.B. Gao, Q.T. Meng, Y.Z. Song, Chin. Phys. B 24 (2015) 013101.
[13] C.X. Zhang, Y.Q. Niu, Q.T. Meng, Chin. Phys. B 23 (2014) 103301.
[14] H.-J. Werner, P.J. Knowles, R. Lindh, et al., MOLPRO, version 2012.1, a package of *ab initio* programs, 2012, see http://www.molpro.net.
[15] K.A. Peterson, C. Puzzarini, Theor. Chem. Acc. 114 (2005) 283.
[16] D.E. Woon, T.H.D. Jr, J. Chem. Phys. 98 (1993) 1358.
[17] H.-J. Werner, P.J. Knowles, J. Chem. Phys. 82 (1985) 5053.
[18] P.J. Knowles, H.-J. Werner, Chem. Phys. Lett. 115 (1985) 259.
[19] H.-J. Werner, P.J. Knowles, J. Chem. Phys. 89 (1988) 5803.
[20] P.J. Knowles, H.-J. Werner, Chem. Phys. Lett. 145 (1988) 514.
[21] A. Berning, M. Schweizer, H.-J. Werner, P.J. Knowles, P. Palmieri, Mol. Phys. 98 (2000) 1823.
[22] J.L. Tilson, W.C. Ermler, Theor. Chem. Acc. 133 (2014) 1564.
[23] R.M. Pitzer, N.W. Winter, J. Phys. Chem. 92 (1988) 3061.
[24] A.B. Alekseyev, H.-P. Liebermann, R.J. Buenker, Recent Advances in Relativistic Molecular Theory, World Scientific, Singapore, 2004.
[25] K. Balasubramanian, Chem. Rev. 89 (1989) 1801.
[26] K. Balasubramanian, Chem. Rev. 90 (1990) 93.
[27] R.J. Le Roy, LEVEL7.7: A computer program for solving the radial schrödinger equation for bound and quasibound levels; university of waterloo, Chemical Physics Research Report, 2005 (CP-661).
[28] C.E. Moore, Atomic Energy Levels, National Bureau of Standard, Washington, DC, 1971.
[29] K.P. Huber, G. Herzberg, Molecular Spectra and Molecular Structure IV, Constants of Diatomic Molecules, Van Nostrand Reinhold, New York, 1979.
[30] M.M. Patel, S.P. Patel, Indian J. Pure Appl. Phys. 4 (1966) 388.
[31] S. Elmoussaoui, N. El-Kork, M. Korek, Comput, Theor. Chem. 1090 (2016) 94.
[32] Y. Liu, H. Zhai, Y. Liu, Eur. Phys. J. D. 69 (2015) 1.
[33] X. Li, B. Minaev, H. Ågren, H. Tian, J. Phys. Chem. C 115 (2011) 20724.
[34] K.K. Das, A.B. Alekseyev, H.-P. Liebermann, G. Hirsch, R.J. Buenker, Chem. Phys. 196 (1995) 395.
[35] I. Boustani, S.N. Rai, H.-P. Liebermann, A.B. Alekseyev, G. Hirsch, R.J. Buenker, Chem. Phys. 177 (1993) 45.
[36] B.F. Minaev, V.A. Minaeva, Y.V. Evtuhov, Int. J. Quantum. Chem. 109 (2009) 500.
[37] B.F. Minaev, N.A. Murugan, H. Ågren, Int. J. Quantum. Chem. 113 (2013) 1847.
[38] H. Li, H. Feng, W. Sun, Y. Xie, H.F. Schaefer, Inorg. Chem. 52 (2013) 6849.
[39] Q. Fan, H. Feng, W. Sun, H. Li, Y. Xie, R.B. King, H.F. Schaefer, New J. Chem. 40 (2016) 8511.
[40] S. Jákó, A. Lupan, A.-Z. Kun, R.B. King, Inorg. Chem. 56 (2017) 351.
[41] H. Ågren, O. Vahtras, B. Minaev, Advances in Quantum Chemistry, Academic Press, 1996.